

14. Zhang, K. *et al.* Structure, alternative splicing, and expression of the human RGS9 gene. *Gene* **240**, 23–34 (1999).

15. Rahman, Z. *et al.* Cloning and characterization of RGS9-2: A striatal-enriched alternatively spliced product of the RGS9 gene. *J Neurosci.* **19**, 2016–2026 (1999).

16. Kooijman, A. C., Houtman, A., Damhof, A. & van Engelen, J. P. Prolonged electro-retinal response suppression (PERRS) in patients with stationary subnormal visual acuity and photophobia. *Doc. Ophthalmol.* **78**, 245–254 (1991).

17. Slep, K. C. *et al.* Structural determinants for regulation of phosphodiesterase by a G protein at 2.0 Å. *Nature* **409**, 1071–1077 (2001).

18. Sandberg, M. A., Pawlyk, B. S. & Berson, E. L. Acuity recovery and cone pigment regeneration after a bleach in patients with retinitis pigmentosa and rhodopsin mutations. *Invest. Ophthalmol. Vis. Sci.* **40**, 2457–2461 (1999).

19. Berson, E. L., Gouras, P. & Gunkel, R. D. Progressive cone degeneration, dominantly inherited. *Arch. Ophthalmol.* **80**, 77–83 (1968).

20. Kooijman, A. C. *et al.* Spectral sensitivity function of the a-wave of the human electroretinogram in the dark-adapted eye. *Clin. Vision Sci.* **6**, 379–383 (1991).

21. Sandberg, M. A. *et al.* Rod and cone function in the Nougaret form of stationary night blindness. *Arch. Ophthalmol.* **116**, 867–872 (1998).

22. Martemyanov, K. A. & Arshavsky, V. Y. Noncatalytic domains of RGS9-1-Gβ5L play a decisive role in establishing its substrate specificity. *J. Biol. Chem.* **277**, 32843–32848 (2002).

23. He, W. *et al.* Modules in the photoreceptor RGS9-1-Gβ5L GTPase-accelerating protein complex control effector coupling, GTPase acceleration, protein folding, and stability. *J. Biol. Chem.* **275**, 37093–37100 (2000).

24. Berson, E. L., Gouras, P. & Gunkel, R. D. Rod responses in retinitis pigmentosa, dominantly inherited. *Arch. Ophthalmol.* **80**, 58–66 (1968).

25. Andreasson, S. O., Sandberg, M. A. & Berson, E. L. Narrow-band filtering for monitoring low-amplitude cone electroretinograms in retinitis pigmentosa. *Am. J. Ophthalmol.* **105**, 500–503 (1988).

26. Marmor, M. F. An international standard for electroretinography. *Doc. Ophthalmol.* **73**, 299–302 (1989).

27. Marmor, M. F. & Zrenner, E. Standard for clinical electroretinography (1994 update). *Doc. Ophthalmol.* **89**, 199–210 (1995).

Supplementary Information accompanies the paper on www.nature.com/nature.

Acknowledgements We thank T. Li, T. McGee and B. Pawlyk for assistance. This study followed the tenets of the Declaration of Helsinki; it was approved by the Human Studies Committees of the authors' institutions and all patients gave their consent before their participation. This work was supported by the NIH, the Foundation Fighting Blindness, Owings Mills, Maryland, and the American Heart Association.

Competing interests statement The authors declare that they have no competing financial interests.

Correspondence and requests for materials should be addressed to T.P.D. (Thaddeus_Dryja@mei.harvard.edu).

Expression and function of orphan nuclear receptor TLX in adult neural stem cells

Yanhong Shi¹, D. Chichung Lie², Philippe Taupin², Kinichi Nakashima^{2,4}, Jasodhara Ray², Ruth T. Yu¹, Fred H. Gage² & Ronald M. Evans^{1,3}

¹Gene Expression Laboratory, ²Laboratory of Genetics, and ³Howard Hughes Medical Institute, The Salk Institute for Biological Studies, 10010 North Torrey Pines Road, La Jolla, California 92037, USA

⁴Department of Cell Fate Modulation, Institute of Molecular Embryology and Genetics, Kumamoto University, 2-2-1, Honjo, Kumamoto 860-0811, Japan

The finding of neurogenesis in the adult brain led to the discovery of adult neural stem cells¹. TLX was initially identified as an orphan nuclear receptor expressed in vertebrate forebrains² and is highly expressed in the adult brain³. The brains of TLX-null mice have been reported to have no obvious defects during embryogenesis⁴; however, mature mice suffer from retinopathies⁵, severe limbic defects, aggressiveness, reduced copulation and progressively violent behaviour^{4,6}. Here we show that TLX maintains adult neural stem cells in an undifferentiated, proliferative state. We show that TLX-expressing cells

isolated by fluorescence-activated cell sorting (FACS) from adult brains can proliferate, self-renew and differentiate into all neural cell types *in vitro*. By contrast, TLX-null cells isolated from adult mutant brains fail to proliferate. Reintroducing TLX into FACS-sorted TLX-null cells rescues their ability to proliferate and to self-renew. *In vivo*, TLX mutant mice show a loss of cell proliferation and reduced labelling of nestin in neurogenic areas in the adult brain. TLX can silence glia-specific expression of the astrocyte marker GFAP in neural stem cells, suggesting that transcriptional repression may be crucial in maintaining the undifferentiated state of these cells.

Expression of TLX in the mouse starts at embryonic day 8 (E8), peaks at E13.5 and decreases by E16, with barely detectable levels at birth. TLX expression increases after birth and is high in the adult brain³. Although TLX-null mice appear grossly normal at birth, mature mice manifest a rapid retinopathy⁵ with reduced cerebral hemispheres^{4,6}. Histologically, adult mutant brains have severely reduced hippocampal dentate gyri, greatly expanded lateral ventricles and reduced olfactory bulbs (Fig. 1a), all of which are active adult neurogenic areas⁷. Behaviourally, TLX mutants show aggressiveness, reduced copulation and progressively violent behaviour^{4,6}. The hypomorphic defects and neurological disorders of the mutant mice suggest that TLX has a role in normal function of the central nervous system (CNS).

Taking advantage of a β-galactosidase (β-gal) reporter, which was knocked into the TLX locus, we examined the expression pattern of TLX in adult brains of heterozygote mice. LacZ staining was distributed sparsely throughout the cortex, but indicated high but dispersed expression of TLX in the subgranular layer of the dentate gyri and clustered expression in the subventricular zone (SVZ; Fig. 1b). Notably, these are the two main sites where adult neural stem cells (NSCs) are located⁷. Previous studies suggested that nestin is a common marker of proliferating CNS progenitors^{8,9}. Immunohistological assessment of brain sections from adult TLX^{+/-} mice showed the colocalization of β-gal and nestin in both the dentate gyri and the SVZ (Fig. 1c), suggesting that TLX is expressed in adult NSCs or progenitor cells.

An emerging concept contends that a subset of the stem cell pool corresponds to a repository of relatively quiescent cells that serve as the source for actively dividing cells¹⁰. To examine whether TLX-expressing cells represent the quiescent or dividing cells, we carried out β-gal and 5-bromodeoxyuridine (BrdU) double staining on brain sections from TLX^{+/-} mice treated with BrdU. The analysis showed that TLX expression corresponds to both BrdU-positive and BrdU-negative cells in the adult germinal zones (dentate gyri and SVZ; Fig. 1d).

Cell sorting was used to isolate TLX-expressing cells to determine their ability to proliferate, self-renew and give rise to both neurons and glia. By using a fluorogenic LacZ substrate, β-gal-positive cells were isolated from TLX^{+/-} forebrains and cultured in N2 medium supplemented with epidermal growth factor (EGF), fibroblast growth factor (FGF) and heparin¹¹. Immunostaining confirmed expression of β-gal in the FACS-sorted cells. The proliferation potential of TLX-positive cells was examined by BrdU labelling of dividing cells. BrdU treatment for 24 h and subsequent immunostaining showed that more than 98% of the β-gal-positive cells were BrdU- and nestin-positive (Fig. 2a).

We next tested the self-renewal capacity of TLX-expressing cells by using clonal analysis¹². Clonal populations were derived from single FACS-sorted, β-gal-positive cells. From a total of 28 single cells, 12 clones developed, 8 of which reached more than 200 cells by day 12; another 4 reached this number by day 25. The clones were dissociated and single cells were plated for a second round of cloning. All of the clones tested were also capable of secondary expansion. A prototypical clonal expansion is shown in Fig. 2b. These results show that TLX-expressing cells comprise a self-renewing population.

We then tested whether TLX cells derived from either primary or secondary clones could be induced to differentiate. Indeed, when examined for the expression of Tuj1 (a neuronal marker), GFAP (an astrocyte marker) and O4 (an oligodendrocyte marker), all three neural cell types with characteristic morphologies were generated upon differentiation (Fig. 2c), indicating that TLX-expressing cells are multipotent. By contrast, the cells isolated from the forebrains of TLX-null littermates failed to proliferate in the same growth conditions (Fig. 2d and Supplementary Fig. 1). Immunostaining showed that, whereas the TLX^{+/-} cells are nestin-positive and GFAP-negative, the TLX^{-/-} cells are nestin-negative but GFAP-

positive, suggesting the spontaneous differentiation of astrocytes (Fig. 2d and Supplementary Fig. 2).

In an attempt to rescue the proliferative defect, FACS-sorted adult TLX^{-/-} (LacZ/LacZ) cells were infected with a lentiviral vector expressing both TLX and green fluorescent protein (GFP). The resulting infected cells were re-sorted on the basis of the internal GFP marker. These infected and selected cells regained the ability to proliferate and could be clonally expanded (Fig. 2e, f). Expression of TLX led to a substantial restoration of cell proliferation, as detected by staining for nestin (Supplementary Fig. 3) and Ki67 (a proliferative marker), and reduced astrocyte differentiation, as detected

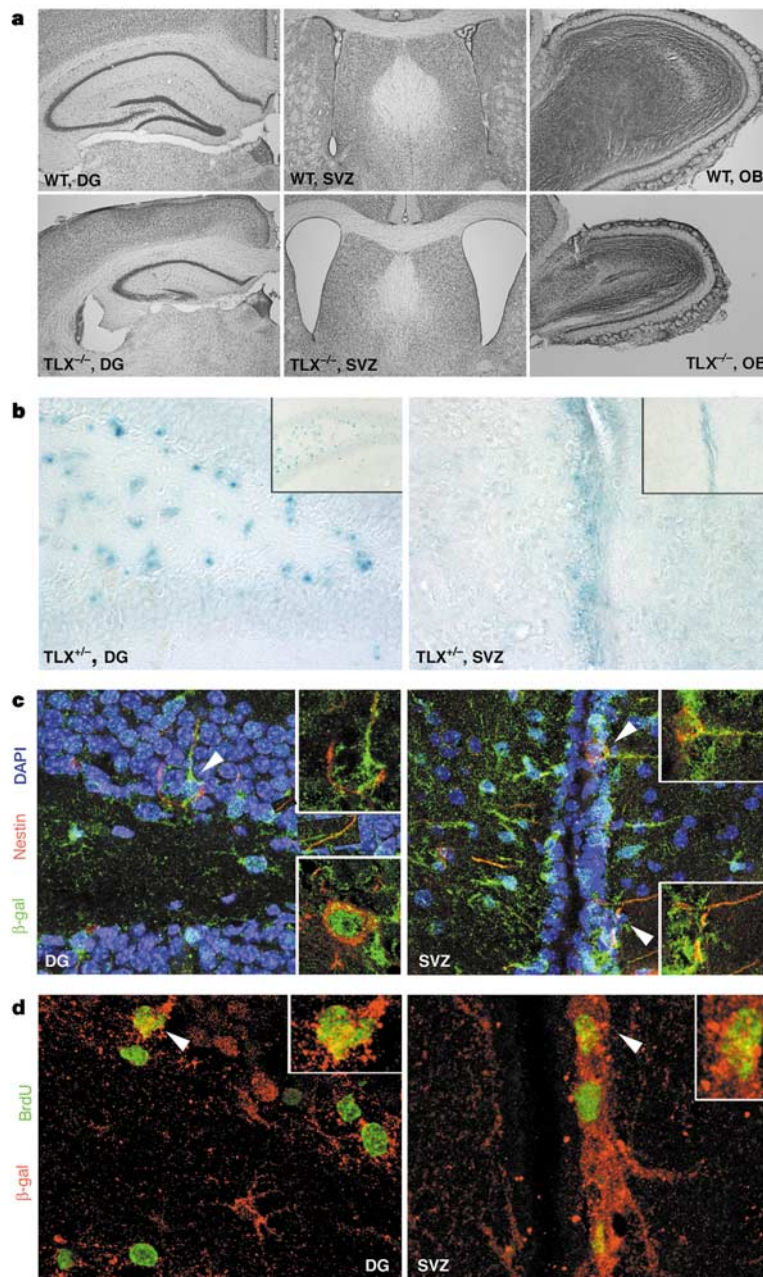


Figure 1 Expression of TLX in adult NSCs. **a**, Nissl staining of brain sections from adult wild-type (WT) and mutant mice. **b**, LacZ staining of dentate gyri and SVZ sections from adult TLX^{+/-} mice. Insets show images at lower magnification. **c**, Co-staining of β -gal and nestin in dentate gyri and SVZ sections from TLX^{+/-} mice. Insets show enlargements of the double-stained cells indicated by arrowheads. The inset in the lower right of the

dentate gyri section shows an example of nestin staining around the nuclei. **d**, Co-staining of β -gal and BrdU in dentate gyri and SVZ sections from TLX^{+/-} mice. Insets show enlargements of the double-stained cells indicated by arrowheads. DG, dentate gyri; OB, olfactory bulbs.

by staining for GFAP (Fig. 2e and Supplementary Fig. 4). By contrast, cells that were infected with a GFP control virus underwent spontaneous differentiation (data not shown). In addition, clonal analysis showed that the cells expressing viral TLX could be clonally expanded from single GFP-positive cells and were both nestin and GFP positive (Fig. 2f). Because the lentivirus-expressed TLX is controlled by the constitutive cytomegalovirus (CMV) promoter, the rescued cells continued to proliferate even under differentiation conditions, as expected (data not shown). Together, these results show that TLX can rescue the undifferentiated, proliferative state of NSCs *in vitro*.

We next examined the transcriptional property of TLX to address how it might contribute to NSC maintenance. When fused to the DNA-binding domain (DBD) of GAL4, TLX strongly repressed a luciferase reporter that was downstream of GAL4 DNA-binding

sites (data not shown). In searching for downstream targets of TLX, a substantial upregulation of GFAP, S100 β and aquaporin 4 (AQP4) was detected in the TLX mutant brains. TLX was expressed in the proliferating NSCs but was switched off upon differentiation, whereas GFAP, S100 β and AQP4 were expressed after differentiation (Fig. 3a). The case for direct regulation was strengthened by the identification of a consensus TLX-binding site, AAGTCA, in the promoters of these genes. Gel shift analysis showed that TLX could specifically bind to these sequences *in vitro* (Fig. 3b and data not shown), suggesting that astrocyte-specific genes are direct downstream targets of TLX repression.

To confirm further this repression by TLX, we carried out reporter assays using a GFAP-promoter-driven luciferase reporter (GFAP-luc)¹³. Leukaemia inhibitory factor (LIF) has been shown to induce astrocyte differentiation and GFAP expression¹³. Co-

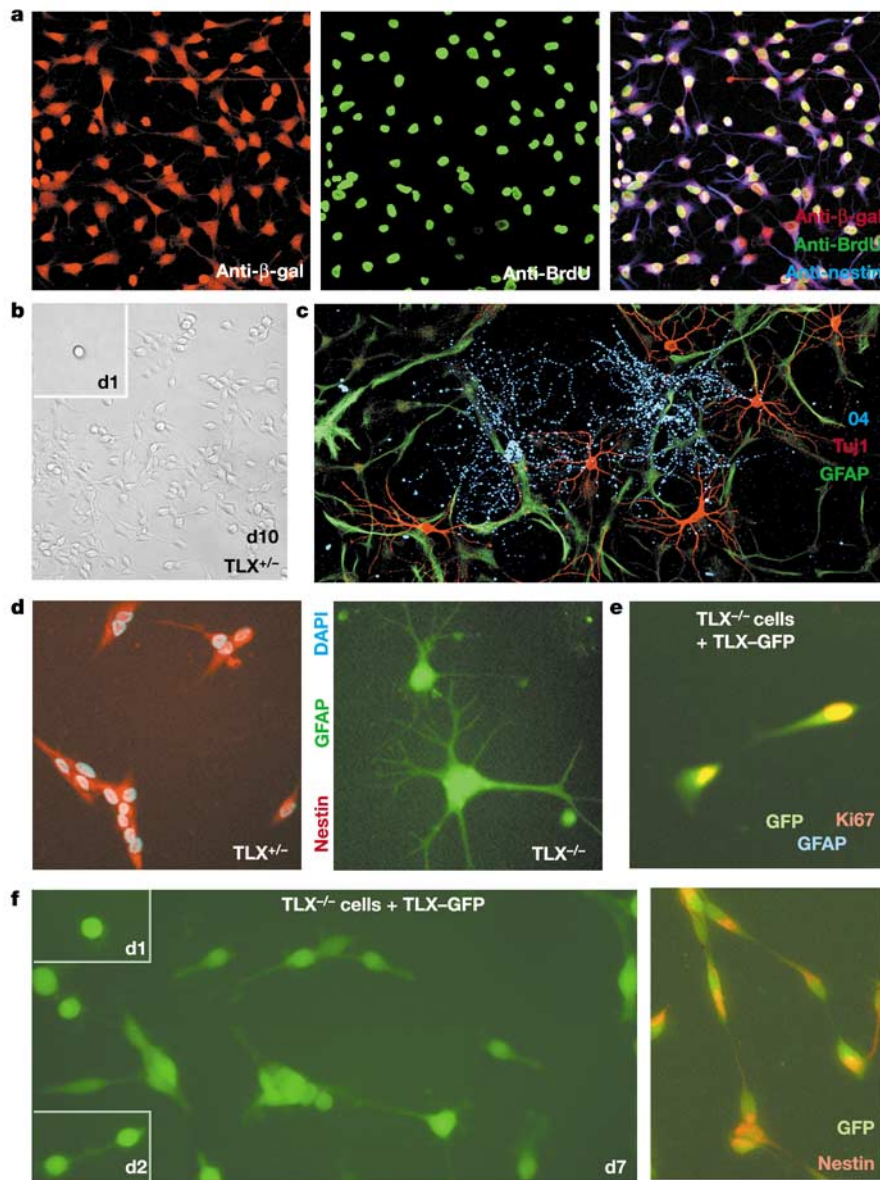


Figure 2 TLX-positive cells are self-renewable and multipotent. **a**, TLX-positive cells were sorted by FACS, treated with BrdU and immunostained for β -gal, BrdU and nestin. **b**, A clonal population of TLX-positive cells at days 1 and 10. **c**, Clonally derived cells were differentiated and stained for Tuj1, GFAP and O4. **d**, Immunostaining of TLX^{+/-} and TLX^{-/-} cells cultured in growth media (see Supplementary Fig. 2 for quantification).

e, Immunostaining of TLX^{-/-} cells expressing TLX-GFP. GFAP staining is negative (see Supplementary Fig. 4 for quantification). **f**, Left, clonal analysis of TLX^{-/-} cells expressing TLX-GFP at days 1, 2 and 7. Right, GFP fluorescence and nestin staining in the cloned cells.

transfection of TLX led to a considerable repression (4.8-fold) of LIF-induced GFAP reporter activity (Fig. 3c), similar to the repression mediated by a dominant-negative variant of STAT3 (ref. 13), which was used as a positive control.

To establish further the role of TLX in the repression of GFAP expression and astrocyte differentiation, we infected NSCs with the TLX-expressing retrovirus. Because it is under a constitutive CMV promoter, the viral TLX remains expressed upon differentiation, in contrast to endogenous TLX, which is downregulated in differentiated cells. As expected, the expression of GFAP and two other astrocyte-specific markers (S100 β and AQP4) was substantially decreased in the cells expressing viral TLX (Fig. 3d). Differentiation of these cells into GFAP-positive astrocytes was reduced proportionately (Fig. 3e). Immunostaining (Fig. 3f) further showed that NSCs with viral TLX expression failed to differentiate into GFAP-positive astrocytes upon treatment with LIF and bone morphogenetic protein 2 (BMP2), a condition favouring astrocyte differentiation. Instead, they continued expressing the neural progenitor marker nestin. Control NSCs infected with GFP virus differentiated into GFAP-positive astrocytes and lost nestin expression under the same conditions. These results further strengthen the argument that TLX is involved in the repression of astrocyte differentiation.

The above analyses suggest that TLX has a role in maintaining the undifferentiated, proliferative state of NSCs. Immunohistochemical assessment of the adult germinal zones detected a marked reduction of nestin-positive cells in both the hippocampal dentate gyri and the SVZ of adult TLX-null mice (Fig. 4a–c), indicating reduced neural precursors in the mutant neurogenic areas. Despite the hypotrophic nature of the mutant brains, an increase in GFAP staining was observed, consistent with the northern analysis (Fig. 3a) and suggesting that there is increased glia differentiation in the brains of mutant mice. TdT-mediated dUTP nick end labelling (TUNEL) assays detected no significant differences in cell death between wild-type and mutant brains (data not shown), suggesting a failure of ongoing cell proliferation or a very early window of cell death.

Next, we examined whether TLX affects cell proliferation in the adult brain. BrdU labelling of adult mice was carried out for 1 week, followed by immunohistochemical assessment. Intensive BrdU labelling was observed along the subgranular zone of the dentate gyri and in the SVZ of the TLX^{+/-} brains, whereas virtually no BrdU labelling was detected in the mutant hippocampus and SVZ (Fig. 4d, e). Quantification of the BrdU-positive cells in the dentate gyri is shown in Fig. 4f. By contrast, as shown by S100 β staining, increased numbers of glia cells were observed in the mutant brains

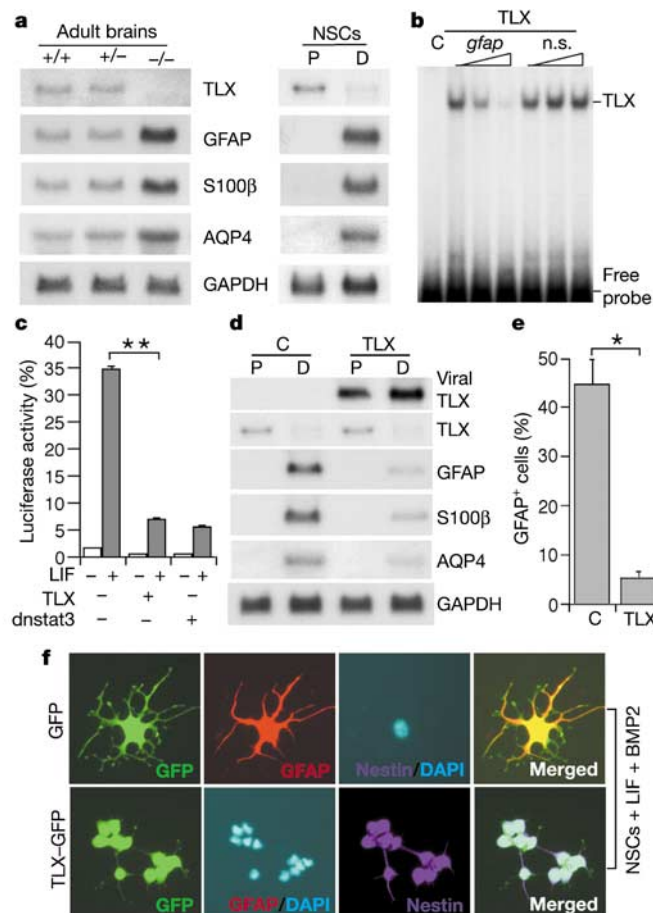


Figure 3 TLX is a transcriptional repressor. **a**, Gene expression in the forebrain of TLX^{+/+}, TLX^{+/-} and TLX^{-/-} mice and in NSCs cultured in proliferation (P) or differentiation (D) conditions analysed by northern blotting. **b**, TLX binds to the GFAP promoter in a gel-shift assay. TLX binding is competed by unlabelled *gfap* but not nonspecific (n.s.) oligos. C, control lysates. **c**, TLX represses GFAP in reporter assays. LIF-induced GFAP-luciferase activity was measured in the absence or the presence of TLX expression. ***P* < 0.0001

by Student's *t*-test. **d**, Gene expression in control (C) or viral TLX-expressing NSCs analysed by northern blotting. P, proliferation; D, differentiation. **e**, Quantification of GFAP-positive astrocytes in control or viral TLX-expressing cells upon differentiation. **P* < 0.001 by Student's *t*-test. **f**, Immunostaining of rat NSCs expressing viral GFP or TLX-GFP.

(Fig. 4g). These results further support our proposal that TLX is essential in maintaining the undifferentiated, proliferative state of stem cells in adult brains.

What are the molecular determinants of adult NSCs? Our characterization of TLX suggests that it may be one of the key regulators that act by controlling the expression of a network of target genes to establish the undifferentiated and self-renewable state of NSCs. The expression of TLX in scattered cells throughout the cortex suggests that it may have another role in addition to its function in the germinal zone. Furthermore, the dominant role in stem cell maintenance that TLX has in the adult is clearly different from its seemingly more modest role in development, although this does not exclude the possibility that the lack of adult NSCs may also

be influenced by developmental functions of TLX. With regard to the persistence of NSCs in the absence of TLX in the adult, the fact that the adult rescue experiment works at all indicates either that a dormant progenitor or NSC population exists or that TLX expression alone can recover a stem cell state in a cell population obtained from the adult germinal region. The characterization of the TLX-expressing cells provides a means to elucidate the molecular and cellular mechanisms underlying stem cell proliferation and differentiation. Furthermore, the use of β -gal-based FACS facilitates the isolation of NSCs from adult brains, which will make it possible to explore clinical applications for transplantability and molecular engineering associated with the treatment of neurodegenerative diseases and brain injuries. □

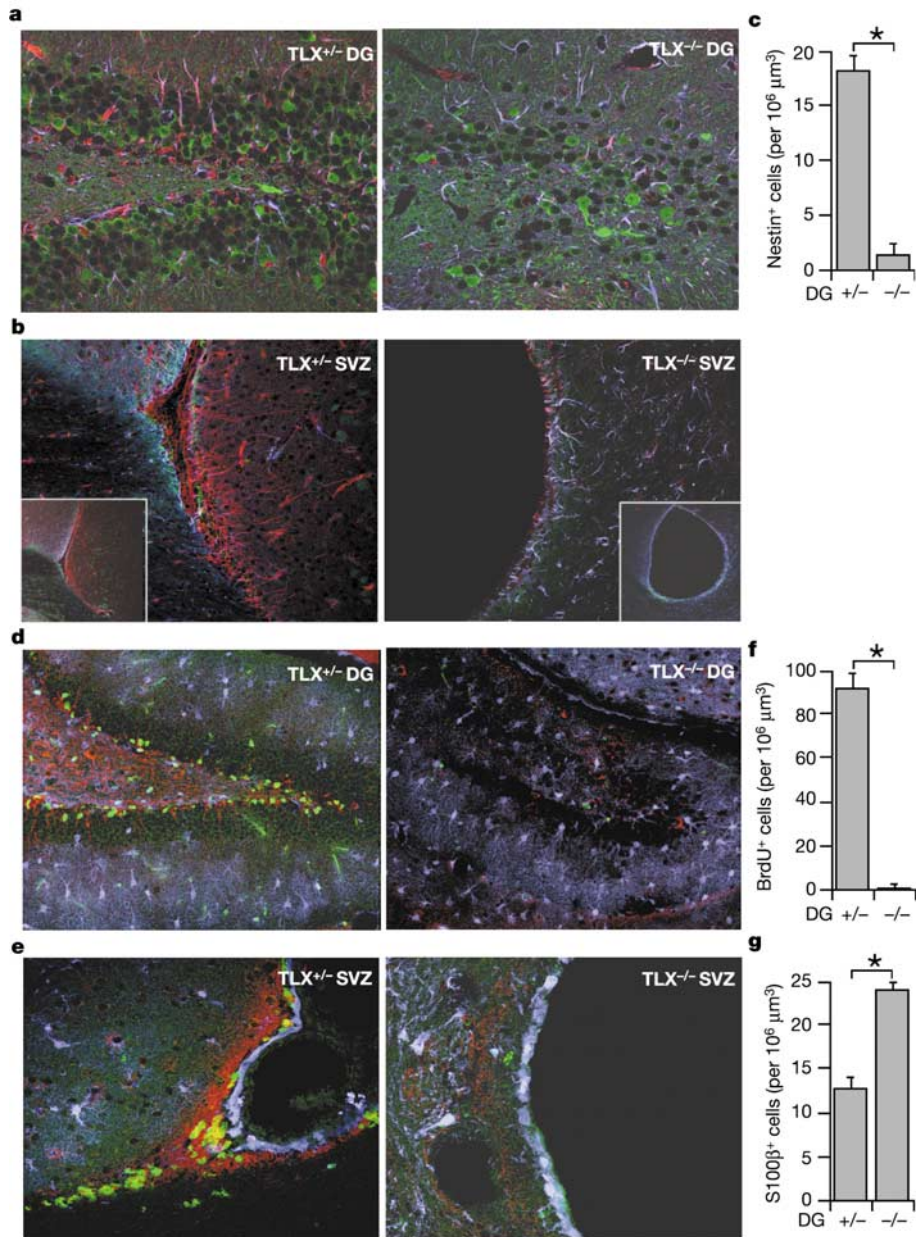


Figure 4 Loss of nestin and BrdU staining in TLX mutant mouse brain. **a**, Coronal dentate gyri sections from the brains of TLX^{+/+} and TLX^{-/-} mice were immunostained for nestin (red), calbindin (green) and GFAP (blue). **b**, Coronal SVZ sections stained for nestin (red), Tuj1 (green) and GFAP (blue). **c**, Quantification of nestin-positive cells in dentate gyri of TLX^{+/+} and TLX^{-/-} mice. **P* < 0.01 by Student's *t*-test. **d, e**, Hippocampal dentate gyri

(**d**) or SVZ (**e**) sections from BrdU-treated TLX^{+/+} and TLX^{-/-} mice were immunostained for BrdU (green), Tuj1 (red) and S100β (blue). **f, g**, Quantification of BrdU-positive cells (**f**) or S100β-positive cells (**g**) in dentate gyri of TLX^{+/+} and TLX^{-/-} mice. **P* < 0.001 by Student's *t*-test.

Methods

Immunocytochemistry and quantification

Immunostaining was carried out on 40-µm free-floating sections¹⁴ or with cultured cells¹² as described. We used the following primary antibodies: rat anti-BrdU (Accurate; diluted 1:250), mouse anti-nestin (PharMingen; 1:1,000), mouse anti-Tuj1 (Bavco; 1:1,000), rabbit anti-S100β (Sigma; 1:500), guinea-pig anti-GFAP (Advance Immuno; 1:500), mouse O4 IgM (a gift from O. Boegler; 1:3), rabbit anti-β-gal (Cortex; 1:2,000), rabbit anti-Ki67 (Novocastra; 1:1,000). BrdU-labelled cells were treated in 1 M HCl at 37 °C for 30 min and visualized by a confocal microscope (BioRad). Quantitative studies were based on four or more replicates. The dentate gyri subgranular areas were traced by semi-automatic stereology using StereoInvestigator software (MicroBrightfield), and volumes were determined by the areas multiplied by the thickness of the sections. Cell densities were calculated by dividing cell numbers by the volume. Statistical analysis was done with Microsoft Excel. For LacZ staining, the 40-µm frozen sections were fixed with glutaraldehyde and paraformaldehyde and stained in 5-bromo-4-chloro-3-indolyl-β-D-galactopyranoside (X-gal; Gibco-BRL) solution containing 20 mM K-ferricyanide, 20 mM ferrocyanide, 0.01% sodium deoxycholate, 0.02% Nonidet P-40 and 2 mM MgCl₂. We used 40X or 10X objectives for the images. Nissl staining was done by using 0.25% Cresyl Violet on 40-µm coronal sections.

Preparation and culture of adult NSC or progenitor cells

Mouse forebrains were minced with scalpels and digested in PPD (Papain, Dispase II and DNase I) solution. Cells were isolated using Percoll gradients¹⁵ and cultured in DMEM F12 medium with 1 mM L-glutamine, N2 supplement (Gibco-BRL), EGF (20 ng ml⁻¹), FGF2 (20 ng ml⁻¹) and heparin (5 µg ml⁻¹). Cells were collected by β-gal-based sorting using fluorescein digalactoside as substrate (Molecular Probes). For differentiation, cells were exposed to N2 supplemented medium containing 5 µM forskolin and 0.5% fetal bovine serum (FBS) for 1 week. Rat NSCs were cultured in N2 medium containing FGF2 (20 ng ml⁻¹) as described¹⁵. Neural differentiation was initiated with N2 supplemented medium containing 1 µM retinoic acid and 0.5% FBS for 4 d. For astrocyte differentiation, cells were cultured in N2 supplemented medium containing 50 ng ml⁻¹ LIF, 50 ng ml⁻¹ BMP2 and 1% FBS. Clonal analysis was done in conditional CCG medium¹². β-gal-positive cells were plated in 96-well plates. Cells were counted 4 h after plating. We monitored wells containing single cells continuously until they reached more than 200 cells.

In vivo BrdU labelling

Eight-week-old mice were injected intraperitoneally once daily with BrdU at 50 mg per kg (body weight) over a 12-d period. Brains were fixed 1 d after the last injection and processed for immunostaining as described¹⁴. Alternatively, BrdU (1 mg ml⁻¹) was administered to mice in their drinking water for 2 weeks, and brain tissues were processed for immunostaining.

Northern blot analysis and gel shift assay

Total RNA from cultured cells or brain tissues was isolated using Trizol reagent (Life Technologies). We carried out northern blot analyses as described¹⁶. Gel shift assay was done as described² using *in vitro* translated TLX and ³²P-labelled GFAP probes.

Transient transfection assays and immunoprecipitation analysis

CV-1 cells were transiently transfected as described¹⁶. Adult rat neural progenitor cells were transfected by using Transit-LT (Mirus). Transfected neural progenitors were treated with solvent or LIF (80 ng ml⁻¹) for luciferase assays. We normalized the luciferase activity of each sample to the β-gal activity in CV-1 cells and the Renilla luciferase activity in progenitor cells. Transfections were done in triplicate at least three times.

Viral production and infection

A TLX-expressing retrovirus was produced by using either an NIT vector and 293gp cells¹⁵ or the pMY vector¹⁷ and Plat-E cells¹⁸. The TLX-expressing lentivirus was produced using pCSC vector¹⁹ and 293T cells. The transgene in the NIT vector is expressed from a minimal CMV promoter containing six tetracycline operators. The transgene in the pMY or pCSC vector is expressed from a CMV promoter and upstream of an IRES GFP marker. The NSCs were infected by incubating with the virus and 2 µg ml⁻¹ polybrene (Sigma). We

selected cells expressing NIT-TLX with 400 µg ml⁻¹ G418. Cells expressing pMY-TLX and pCSC-TLX were sorted by the IRES GFP marker.

Received 28 July; accepted 9 October 2003; doi:10.1038/nature02211.

- Gage, F. H. Mammalian neural stem cells. *Science* **287**, 1433–1438 (2000).
- Yu, R. T., McKeown, M., Evans, R. M. & Umeson, K. Relationship between *Drosophila* gap gene tailless and a vertebrate nuclear receptor Tlx. *Nature* **370**, 375–379 (1994).
- Monaghan, A. P., Grau, E., Bock, D. & Schutz, G. The mouse homolog of the orphan nuclear receptor tailless is expressed in the developing forebrain. *Development* **121**, 839–853 (1995).
- Monaghan, A. P. *et al.* Defective limbic system in mice lacking the tailless gene. *Nature* **390**, 515–517 (1997).
- Yu, R. T. *et al.* The orphan nuclear receptor Tlx regulates Pax2 and is essential for vision. *Proc. Natl Acad. Sci. USA* **97**, 2621–2625 (2000).
- Chiang, M. Y. & Evans, R. M. *Reverse Genetic Analysis of Nuclear Receptors, RXRg, RARb, and TLX in Mice* (Dissertation, Univ. California, San Diego, 1997).
- Gage, F. H. Neurogenesis in the adult brain. *J. Neurosci.* **22**, 612–613 (2002).
- Lendahl, U., Zimmerman, L. B. & McKay, R. D. CNS stem cells express a new class of intermediate filament protein. *Cell* **60**, 585–595 (1990).
- Reynolds, B. A., Tetzlaff, W. & Weiss, S. A multipotent EGF-responsive striatal embryonic progenitor cell produces neurons and astrocytes. *J. Neurosci.* **12**, 4565–4574 (1992).
- Doetsch, F., Petreanu, L., Caille, I., Garcia-Verdugo, J. M. & Alvarez-Buylla, A. EGF converts transit-amplifying neurogenic precursors in the adult brain into multipotent stem cells. *Neuron* **36**, 1021–1034 (2002).
- Allen, D. M. *et al.* Ataxia telangiectasia mutated is essential during adult neurogenesis. *Genes Dev.* **15**, 554–566 (2001).
- Taupin, P. *et al.* FGF-2-responsive neural stem cell proliferation requires CCG, a novel autocrine/paracrine cofactor. *Neuron* **28**, 385–397 (2000).
- Nakashima, K. *et al.* Synergistic signaling in fetal brain by STAT3–Smad1 complex bridged by p300. *Science* **284**, 479–482 (1999).
- Lie, D. C. *et al.* The adult substantia nigra contains progenitor cells with neurogenic potential. *J. Neurosci.* **22**, 6639–6649 (2002).
- Palmer, T. D., Markakis, E. A., Willhoite, A. R., Safar, F. & Gage, F. H. Fibroblast growth factor-2 activates a latent neurogenic program in neural stem cells from diverse regions of the adult CNS. *J. Neurosci.* **19**, 8487–8497 (1999).
- Shi, Y. *et al.* Sharp, an inducible cofactor that integrates nuclear receptor repression and activation. *Genes Dev.* **15**, 1140–1151 (2001).
- Misawa, K. *et al.* A method to identify cDNAs based on localization of green fluorescent protein fusion products. *Proc. Natl Acad. Sci. USA* **97**, 3062–3066 (2000).
- Morita, S., Kojima, T. & Kitamura, T. Plat-E: an efficient and stable system for transient packaging of retroviruses. *Gene Ther.* **7**, 1063–1066 (2000).
- Miyoshi, H., Blomer, U., Takahashi, M., Gage, F. H. & Verma, I. M. Development of a self-inactivating lentivirus vector. *J. Virol.* **72**, 8150–8157 (1998).

Supplementary Information accompanies the paper on www.nature.com/nature.

Acknowledgements We thank G. Cabrera, S. Tjep, M. Nelson, H. Juguilon, J. Havstad, B. Miller, R. Summers, A. Consiglio, A. Huynh, L. Moore, A. Dearie and H. Lansford for technical help; M. L. Gage for editing; E. Stevens and E. Ong for administrative assistance; C. Zhang for comments on the manuscript; R. Marr and I. Verma for the lentiviral vector; and T. Kitamura for the pMY vector and Plat-E cells. Y.S. is a fellow of the Susan G. Komen Breast Cancer Foundation. D.C.L. was supported by the Deutsche Forschungsgemeinschaft. P.T. was supported by the Pasarow Foundation. K.N. was supported by a Japan Society for the Promotion of Science (JSPS) Postdoctoral Fellowship for Research Abroad. R.M.E. is an Investigator of the Howard Hughes Medical Institute at the Salk Institute and March of Dimes Chair in Molecular and Developmental Biology. F.H.G. is the Adler Professor of Age-Related Neurodegenerative Diseases. This work was supported by the Howard Hughes Medical Institute, the NIH, the Christopher Reeve Paralysis Foundation, the National Institutes of Aging, the Michael J. Fox Foundation, Project ALS and the Lookout Fund.

Competing interests statement The authors declare that they have no competing financial interests.

Correspondence and requests for materials should be addressed to R.M.E. (evans@salk.edu) or F.H.G. (gage@salk.edu).